

## The reduction of magnetic reconnection outflow jets to sub-Alfvénic speeds

Colby C. Haggerty, Michael A. Shay, Alexandros Chasapis, Tai D. Phan, James F. Drake, Kittipat Malakit, Paul A. Cassak, and Rungployphan Kieokaew

Citation: *Physics of Plasmas* **25**, 102120 (2018); doi: 10.1063/1.5050530

View online: <https://doi.org/10.1063/1.5050530>

View Table of Contents: <http://aip.scitation.org/toc/php/25/10>

Published by the [American Institute of Physics](#)

---

---

**PHYSICS TODAY**

WHITEPAPERS

### MANAGER'S GUIDE

Accelerate R&D with  
Multiphysics Simulation

READ NOW

PRESENTED BY

 **COMSOL**

# The reduction of magnetic reconnection outflow jets to sub-Alfvénic speeds

Colby C. Haggerty,<sup>1,2,a)</sup> Michael A. Shay,<sup>2</sup> Alexandros Chasapis,<sup>2</sup> Tai D. Phan,<sup>3</sup> James F. Drake,<sup>4</sup> Kittipat Malakit,<sup>5</sup> Paul A. Cassak,<sup>6</sup> and Rungployphan Kieokaew<sup>7</sup>

<sup>1</sup>*Department of Astronomy and Astrophysics, University of Chicago, Chicago, Illinois 60637, USA*

<sup>2</sup>*Department of Physics and Astronomy, Bartol Research Institute, University of Delaware, Newark, Delaware 19716, USA*

<sup>3</sup>*Space Sciences Laboratory, University of California, Berkeley, California 94720, USA*

<sup>4</sup>*Institute for Research in Electronics and Applied Physics, University of Maryland, College Park, Maryland 20742, USA*

<sup>5</sup>*Department of Physics, Faculty of Science and Technology, Thammasat University, Pathum Thani 12120, Thailand*

<sup>6</sup>*Department of Physics and Astronomy, West Virginia University, Morgantown, West Virginia 26506, USA*

<sup>7</sup>*CGAFD, Mathematics, CEMPS, University of Exeter, Exeter EX4 4QF, United Kingdom*

(Received 31 July 2018; accepted 8 October 2018; published online 31 October 2018)

The outflow velocity of jets produced by collisionless magnetic reconnection is shown to be reduced by the ion exhaust temperature in fully kinetic particle in cell simulations and *in situ* satellite observations. We derive a scaling relationship for the outflow velocity based on the upstream Alfvén speed and the parallel ion exhaust temperature, which is verified in kinetic simulations and observations. The outflow speed reduction is shown to be due to the firehose instability criterion, and so, for large enough guide fields, this effect is suppressed and the outflow speed reaches the upstream Alfvén speed based on the reconnecting component of the magnetic field. *Published by AIP Publishing.* <https://doi.org/10.1063/1.5050530>

## I. INTRODUCTION

Magnetic reconnection is a plasma process that efficiently releases energy stored in magnetic fields and generates fast plasma jets.<sup>1</sup> Reconnection occurs at thin current sheets where the direction of the magnetic field changes over a small spatial scale. During reconnection, the frozen-in condition of magnetohydrodynamics is broken and field lines effectively “break” and cross connect, creating stretched field lines, which relax via the tension force. This contraction of the field line generates bulk plasma outflow away from the location where this breaking occurred (called the x-line) with a speed expected to reach the Alfvén speed based on the inflowing plasma parameters and the changing component of the magnetic field.<sup>2</sup>

Outflow jets are one of the most recognizable features of reconnection. They have been repeatedly observed in simulations and laboratory and satellite observations (e.g., Paschmann *et al.*,<sup>3</sup> Sonnerup,<sup>4</sup> Sato and Hayashi,<sup>5</sup> Birn and Hones,<sup>6</sup> and Stenzel *et al.*<sup>7</sup>). Observational events typically require a jet detection to be classified as reconnection. However, in both simulations and observations, the magnitude of the outflow speed is often found to be significantly less than the Alfvén speed (e.g., Paschmann *et al.*,<sup>8</sup> Phan *et al.*,<sup>9</sup> Gosling *et al.*,<sup>10</sup> Liu *et al.*,<sup>11</sup> and Haggerty *et al.*<sup>12</sup>). A significant amount of the converted magnetic energy is transferred into the outflow jets,<sup>13–18</sup> and the magnitude of the jet velocities has important consequences for many different collisionless plasma systems where reconnection occurs (e.g., dipolarization fronts,<sup>19,20</sup> in thermal<sup>12,21</sup> and non-thermal particle energization,<sup>22,23</sup> and potentially many others). The

ability to predict the effects of reconnection on any plasma system requires the accurate prediction of outflow jets, and this work offers a simple scaling prediction consistent with observations and simulations and is thus a critical step in a predictive description of magnetic reconnection.

In this work, we show that the firehose instability criterion being reached in the exhaust<sup>11,24</sup> reduces the outflow velocity in nearly anti-parallel reconnection events and derive a prediction for the reduction. A relationship is derived by matching the anisotropic Rankine-Hugoniot conditions across the edge of the reconnection exhaust boundary. The prediction is tested using 81 particle-in-cell (PIC) reconnection simulations and 14 previously published observational events and is found to agree remarkably well. Finally, we discuss the implications of this result, and its importance to understanding how released magnetic energy is partitioned during reconnection.

## II. SIMULATIONS AND OBSERVATIONS

To study why the outflow velocity is less than the Alfvén speed, we examine 81 reconnection simulations [56 where the two reconnecting field lines are separated by more than 135° (nearly anti-parallel) and 25 where they are separated by some smaller angle (in this work <135°) (guide field)] performed using the kinetic-PIC code P3D Zeiler *et al.*<sup>25</sup> In the simulations, magnetic field strengths and particle number densities are normalized to arbitrary characteristic values  $B_0$  and  $n_0$ , respectively. Lengths are normalized to the ion inertial length  $d_{i0} = c/\omega_{pi0}$  at the reference density  $n_0$ . Time is normalized to the ion cyclotron time  $\Omega_{ci0}^{-1} = (eB_0/m_i c)^{-1}$ . Speeds are normalized to the Alfvén speed  $c_{A0} = \sqrt{B_0^2/(4\pi m_i n_0)}$ . Electric fields and temperatures are normalized to  $E_0 = c_{A0} B_0/c$  and

<sup>a)</sup>Electronic mail: CHaggerty@UChicago.edu

$T_0 = m_i c_{A0}^2$ , respectively. The coordinate system is in “simulation coordinates,” meaning that the reconnection outflows are along  $\hat{x}$  and the inflows are along  $\hat{y}$ .

Simulations are performed in a periodic domain with size and grid scale varied based on simulation and inflow parameters. The reconnection simulation parameters are described in detail in two previous publications<sup>12,17</sup> A range of reconnection magnetic fields  $B_r$ , upstream densities  $n_{up}$ , and upstream ion and electron temperatures  $T_{i,up}$  and  $T_{e,up}$  are used. The parameters for the simulations are shown in the [supplementary material](#).

In each simulation, we take a trapezoidal region from 5 to 20  $d_i$  downstream of the x-line bounded by the exhaust boundary in order to calculate the average parallel ion exhaust temperature. The outflow velocity is taken as the asymptotic  $E \times B$  velocity at the midplane sufficiently far downstream of the x-line. Further details about the calculation of these values are detailed in the work of Haggerty *et al.*<sup>12</sup>

Along with simulations, we also examine 14 previously published observed reconnection events.<sup>10,26–33</sup> These events were measured in several different plasma systems, including the solar wind, the magnetosheath, and the magnetotail.

In Figs. 1(a) and 1(b), the asymptotic  $E \times B$  outflow velocity is plotted against the upstream Alfvén speed based on the reconnecting magnetic field  $c_{Ar}$  with a dashed black line corresponding to a slope of 1 for the simulations and observations, respectively. For the guide field cases (green circles), there is good agreement between the outflow velocity and the upstream Alfvén speed based on the reconnecting magnetic field. However, for every nearly anti-parallel simulation and observation (red white and blue triangles) irrespective of the initial conditions, the outflow velocity is less than the Alfvén speed. The difference between the outflow and the Alfvén speed also varies dramatically between different events. There are numerous cases where the outflow is almost as large as Alfvén speed, and there are also many events where the outflow is an order of magnitude smaller than the Alfvén speed. It is clear that in the absence of a guide field, the outflow velocity can be significantly reduced.

The reduction of the outflow velocity is linked in some way to the upstream ion beta  $\beta_i$  based on the reconnecting component of the upstream magnetic field indicated by the triangle’s color in Fig. 1(a). As  $\beta_i$  goes to zero (blue triangles), the outflow approaches the Alfvén speed, and as  $\beta_i$  becomes larger (red triangles), the outflow velocity is reduced. This suggests that the ion upstream thermal velocity relative to the upstream Alfvén speed reduces the outflow. This is explored in Sec. III where we have analyzed the effects of the firehose instability in reconnection exhausts. In Sec. III, a theory for this relationship is derived.

### III. THEORY

Using double adiabatic theory<sup>34</sup> for a parallel propagating shear Alfvén wave, the dispersion relationship can be shown to be  $\omega^2 = \frac{k^2}{m_i n} \left( \frac{B^2}{4\pi} + P_\perp - P_\parallel \right)$  where  $P_\parallel$  and  $P_\perp$  are the sum of the ion and electron thermal pressures parallel and perpendicular to the local magnetic field line.<sup>35</sup> For an isotropic system, the relationship becomes  $\omega = c_A k$  with the phase velocity equal to the Alfvén speed. There is clearly a

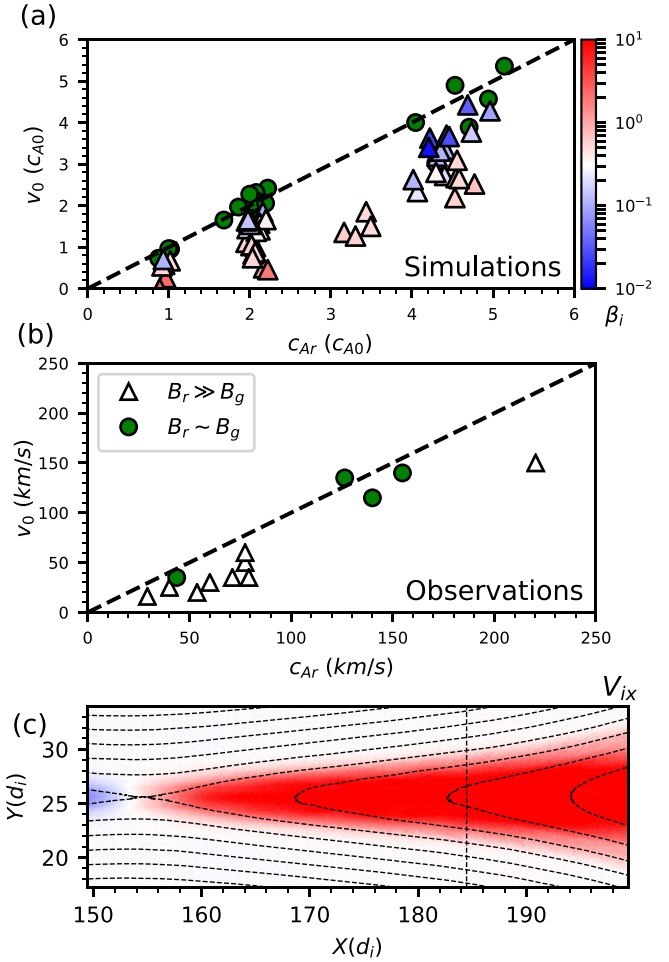


FIG. 1. (a) and (b) The asymptotic  $E \times B$  outflow velocity  $v_0$  against the upstream Alfvén speed based on the reconnecting magnetic field  $c_{Ar}$  for 81 different PIC simulations (a) and 14 previously published observational events (b). The green circles correspond to simulations with a guide field comparable to the reconnecting field, and the blue/white/red triangles correspond to nearly anti-parallel reconnection events. (c) 2D color plot of the ion outflow velocity  $v_{ix}$  for an example simulation with contours of the magnetic field plotted in black dashed lines. The vertical dashed black line shows where the cut is taken for Fig. 2(a). This is simulation 693 in the table in the [supplementary material](#).

regime where the right side is negative, and the wave is unstable. This occurs when  $P_\parallel > \frac{B^2}{4\pi} + P_\perp$  or equivalently when  $\epsilon$  defined as  $\epsilon = 1 + 4\pi(P_\perp - P_\parallel)/B^2 < 0$  and is referred to as the firehose instability. Conceptually, this instability can be interpreted as an effective centrifugal force from particles traveling along curved magnetic field lines due to  $P_\parallel$  that beats the tension force trying to straighten out the field line. When  $\epsilon \rightarrow 0$ , the pressure force is completely counter-balancing the tension in the magnetic field line, and the field line cannot accelerate the plasma.

Previous work has accounted for anisotropic pressures and has shown that the tangential flow across a rotational discontinuity (RD) is given by

$$\mathbf{v}_{t2} - \mathbf{v}_{t1} = \sqrt{\frac{n_1 \epsilon_1}{4\pi m_i}} \left( \frac{\mathbf{B}_{r1}}{n_1} - \frac{\mathbf{B}_{r2}}{n_2} \right). \quad (1)$$

This prescription can be applied to the boundary of a reconnection exhaust to give a prediction for the outflow

velocity.<sup>4,36</sup> This is done by taking the “1” location to be upstream of the reconnection exhaust, and the “2” location where the reconnecting magnetic field goes to zero, as well as taking the tangential direction parallel to the outflow and the normal along the inflow direction. Assuming that the upstream pressure is isotropic, the outflow is predicted to be the upstream Alfvén speed based on the reconnecting component of the magnetic field,  $v_0 = \frac{B_r}{\sqrt{4\pi m_i n_{i0}}} = c_{Ar}$ . In Figs. 1(a) and 1(b), it is clear that for both simulations and observations with a guide field (denoted by green circles), the outflow agrees with this prediction. However, for nearly anti-parallel events, there is significant deviation from what theory predicts.

This effect can be seen even more clearly in Figs. 2(a) and 2(b), which show cuts of the ion outflow velocity normalized to the upstream Alfvén speed (solid blue line), the ion firehose parameter (solid black line), and the prediction (red dashed line) plotted along the inflow direction  $30d_{i0}$  downstream of the x-line for an anti-parallel and guide field simulation, a and b, respectively. For both the guide field and anti-parallel case, there is a deviation between the ion outflow and the RD prediction along the edge of the exhaust associated with an electron return current required that generates the hall magnetic field structure;<sup>37,38</sup> however, farther into the exhaust outflow velocity agrees well with the ion outflow in the guide field simulation but not in the anti-parallel case. In the guide field case, the jet speed continues to increase towards the center of the exhaust, reaching the upstream Alfvén speed at the midplane. In the anti-parallel cut, precisely at the region where  $\epsilon \rightarrow 0$ , the outflow velocity stops increasing and flattens off to a value significantly less than 1. This suggests that the firehose instability is potentially responsible for limiting the outflow velocity.

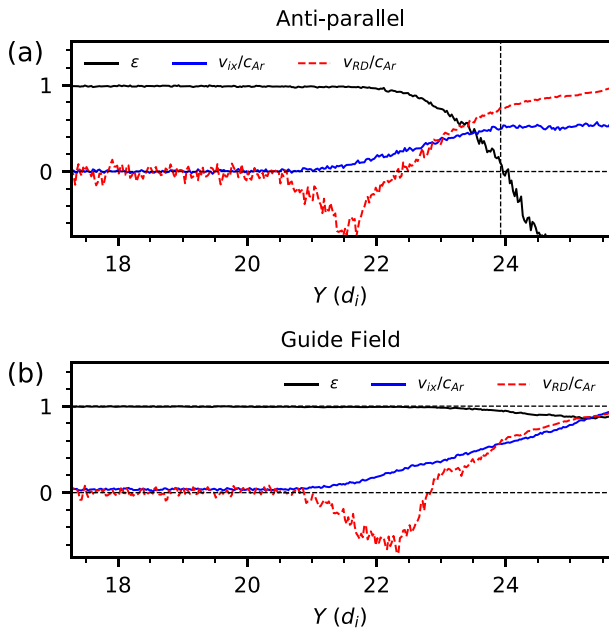


FIG. 2. (a) A cut of the ion firehose parameter  $\epsilon$  (solid black line), ion outflow velocity normalized to the upstream Alfvén speed  $v_{ix}/c_{Ar}$  (solid blue line), and the out flow predicted by Eq. (1) normalized to the upstream Alfvén speed along the x direction for an anti-parallel [(a) simulation 693] and guide field [(b) simulation 708] simulation. Each cut is taken  $30d_i$  downstream of the x-line, as is demonstrated in Fig. 1(c) for simulation 693.

To derive a prediction for the scaling of the outflow velocity, we analyze the anisotropic Rankine-Hugoniot jump conditions across the reconnection exhaust boundary layer.<sup>36</sup> Note that the exhaust boundary is different from the separatrix which is the topological boundary defined by the field line passing through the x-point; the exhaust boundary is a line quasi-parallel to, but contained within, the separatrix which separates the hot, fast flowing exhaust plasma and the cooler, slowly inward convecting plasma [diagrammed in Fig. 3(a)]. The jump conditions are<sup>11,24,36</sup>

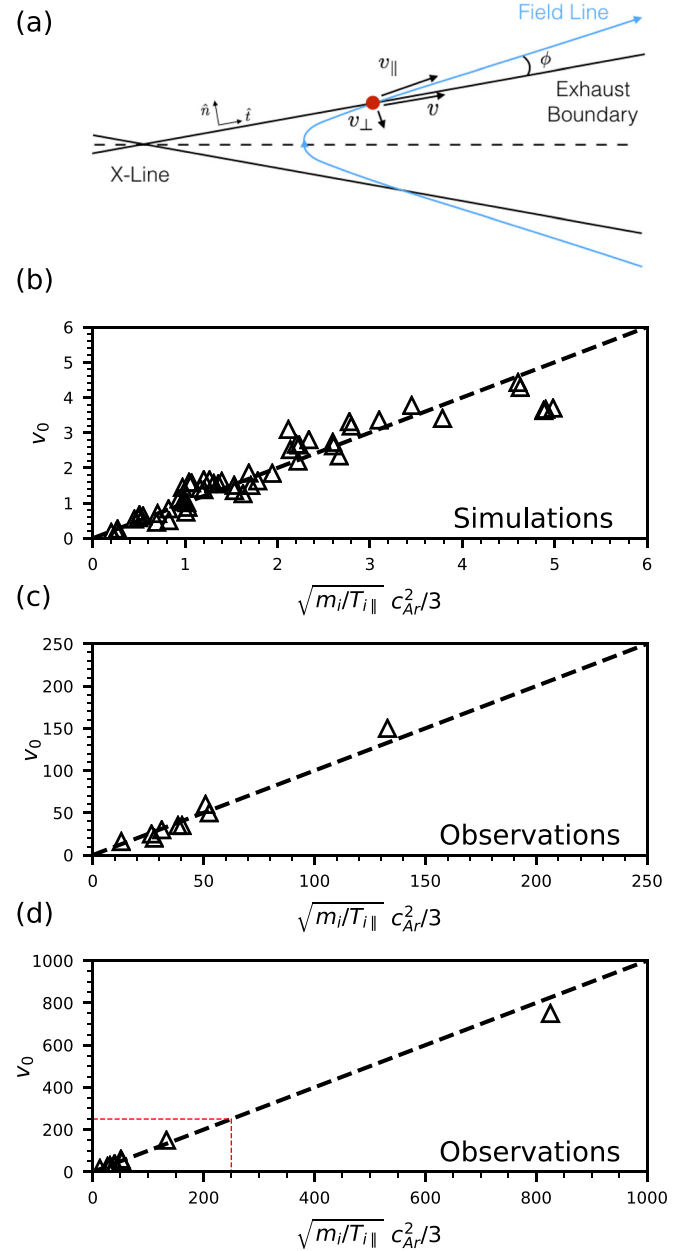


FIG. 3. (a) Diagram of an accelerated ion’s (red circle) motion relative to the exhaust boundary (black line) and the magnetic field (blue curve). (b)–(d) The asymptotic  $E \times B$  outflow velocity versus the outflow prediction described in Eq. (12) for PIC simulations (b) and for observations (c) and (d) for nearly anti-parallel events. Panel (d) is the same as (c), but it includes a magnetotail event with an outflow velocity so large that it obscures the data from the other events. The red dashed box shows the limits of panel (c) for comparison.

$$[B_n]_d^u = 0, \quad (2)$$

$$[nv_n]_d^u = 0, \quad (3)$$

$$\left[ m_i n v_n v_t - \epsilon \frac{B_n B_t}{4\pi} \right]_d^u = 0, \quad (4)$$

where  $[\dots]_d^u$  represent the difference between the upstream and downstream of the exhaust boundary and the subscripts  $n$  and  $t$  correspond to the directions normal and tangential to the exhaust boundary, respectively, shown in Fig. 3(a). By comparing at a point upstream of the reconnection and the location where  $\epsilon$  goes to zero in the exhaust, we find from Eqs. (2) and (4) that the outflow velocity (which at this location  $v_0 \approx v_{td}$ ) satisfies the relationship

$$(nv_n)_d v_0 = (nv_n v_t)_u - \epsilon_u \frac{B_n B_{tu}}{4\pi m_i}. \quad (5)$$

This equation can be further simplified by noting that the upstream inflowing velocity  $v_{nu}$  and the upstream flow tangential to the exhaust boundary  $v_{tu}$  are both very small quantities compared to either the outflow velocity or the upstream Alfvén speed. The first term of the right hand side of Eq. (5) can, therefore, be ignored and the outflow velocity becomes

$$v_0 = -\epsilon_u \frac{B_n B_{tu}}{4\pi m_i n_u v_{nu}}, \quad (6)$$

where we have used  $n_d v_{nd} = n_u v_{nu}$  from Eq. (3).

Figure 3(a) shows a schematic of a magnetic field line threading through the exhaust boundary layer at a small angle  $\phi$ . The magnetic field and bulk flow can then be rewritten in terms of this angle

$$B_{tu} = B \cos \phi \approx B_r, \quad (7)$$

$$B_n = B \sin \phi \approx B_r \phi, \quad (8)$$

$$v_{nu} = -v_{E \times B} \cos \phi \approx -v_{E \times B}, \quad (9)$$

where  $v_{E \times B}$  is the  $E \times B$  velocity of the inflowing plasma. Substituting Eqs. (7)–(9) into Eq. (6), we find

$$v_0 = \epsilon_u c_{Ar}^2 \frac{\phi}{v_{E \times B}}. \quad (10)$$

In Fig. 3(a), we show a diagram of ion population (denoted by the red circle) that has been accelerated by the Fermi mechanism and is now traveling out of the exhaust along a field line. In the magnetic field coordinate system, the ion is traveling with a parallel and perpendicular velocity ( $v_{\parallel}$  and  $v_{\perp}$  respectively). This population of ions entered the reconnection exhaust closer to the x-line and is now traveling away from the midplane on the upper half of the exhaust. These ions mix with the inflowing plasma and form the density enhancement associated with the exhaust boundary layer. Since these ions make up this boundary, the population's relative motion should be parallel to the boundary. This implies that  $\phi \approx \tan \phi = v_{\perp}/v_{\parallel}$ . Using the  $E \times B$  velocity for the perpendicular velocity and substituting this into

Eq. (10), we find that the outflow velocity should be  $v_0 = \epsilon_u c_{Ar}^2 / v_{\parallel}$  where  $v_{\parallel}$  is the parallel velocity component of the ions flowing away from the midplane at the leading edge of the exhaust boundary.

It is not clear exactly what value  $v_{\parallel}$  should have. In the limit where the inflowing ion thermal velocity is much larger than the Alfvén speed, only half of the inflowing population would enter the exhaust (the half with a parallel velocity pointing towards the midplane) and then  $v_{\parallel} \sim \sqrt{T_i/m_i}$ . In this limit as the upstream ion temperature increases, the outflow velocity becomes much smaller than the Alfvén speed. In the limit of cold inflowing ions, if we neglect the effect of the potential associated with electron trapping,<sup>12,39,40</sup> the parallel velocity is simply  $v_{\parallel} = 2v_0$ . Using this, the outflow velocity should be  $v_0 = c_A / \sqrt{2}$ . This can be interpreted as an upper bound for the outflow velocity in anti-parallel reconnection. Using this prediction for the outflow with the ion heating predicted by Eq. (8) in the work of Drake *et al.*,<sup>13</sup> the total ion heating is  $\Delta T_i = .167 m_i c_A^2$  which is within 20% of the reported heating identified in observations and simulations.<sup>12,41</sup> The behavior in both of these limits and the physical interpretation of this velocity suggests that  $v_{\parallel} \propto \sqrt{T_{i\parallel}/m_i}$ , where  $T_{i\parallel}$  is the parallel ion temperature in the exhaust. Note that this temperature is the parallel ion exhaust temperature and, thus, includes both the initial upstream temperature and the additional temperature generated during reconnection. Furthermore, in the cold upstream, potential free limit  $T_{i\parallel} \sim \Delta T_{i\parallel} = v_{\parallel}^2$ , and in the hot upstream limit  $T_{i\parallel} \sim T_{i,up} \sim v_{\parallel}^2$ . From this, we find

$$v_0 \propto \epsilon_u \frac{c_{Ar}^2}{\sqrt{T_{i\parallel}/m_i}}. \quad (11)$$

This scaling prediction agrees with what is found in Fig. 1(a). When the reconnecting plasma's ion beta is small,  $T_{i\parallel} \sim \Delta T_{i\parallel} \sim m_i v_0^2$ , so using this in Eq. (11) implies  $v_0 \sim c_{Ar}$ , which is in agreement with the blue triangles lying on a line with the same slope. When the plasma has a larger initial ion beta,  $T_{i\parallel} \sim T_{i,up}$  and so Eq. (11) becomes  $v_0 \propto c_{Ar} / \sqrt{\beta_i}$ , which agrees with Fig. 1(a) as well.

Because  $T_{i\parallel}$  includes the ion heating generated during reconnection and the heating is linked to the outflow velocity,<sup>12,13</sup> this relationship does not uniquely determine the outflow velocity. To explicitly link the upstream ion temperature and the outflow would require incorporating a prediction for the ion heating which ultimately depends not only on the outflow but also the electron temperature/heating and the associated parallel potential, which is beyond the scope of this work. Equation (11), however, provides an important link between temperature and exhaust velocity which can be tested experimentally and numerically. It may ultimately form the basis of a complete predictive theory for both outflow velocities and heating. This is an important outstanding problem in reconnection and plasma physics and should be addressed in the future.

To test Eq. (11), we examine nearly anti-parallel simulations and observations shown in Figs. 1(a) and 1(b). In Fig. 3, the outflow velocity measured in nearly anti-parallel simulations (b) and observations (c and d) is plotted against the

formula given in Eq. (11) using 1/3 as the proportionality constant. The agreement between the theory and measured outflow velocity is remarkable. Both simulation and observation data points now lie along a single line with the same empirical factor of 1/3 for both, whereas before the inclusion of the ion temperature term events would have a range of different velocities for the same prediction [i.e., the spread in  $v$  in Fig. 1(a)].

In Fig. 3(d), the same data are shown as in Fig. 3(c) with an extra observational event. This event occurred in Earth's magnetotail and was studied extensively by Hietala *et al.*<sup>31</sup> The magnitude of the upstream Alfvén speed in this event is so large that it dwarfs all the other events. The red dashed lines show the limits of Fig. 3(c) to emphasize this point. In this event, the outflow velocity was significantly reduced from the Alfvén speed by as much as 400 km/s; its speed is consistent with the theory presented here. Putting in the empirical multiplicative factor of 1/3 gives an accurate prediction for the outflow velocity  $v_0$  in nearly anti-parallel symmetric magnetic reconnection

$$v_0 = \frac{\epsilon_u}{3} \frac{c_{Ar}^2}{\sqrt{T_{i\parallel}/m_i}}. \quad (12)$$

In the presence of a sufficiently strong guide field, the outflow velocity agrees with the Hudson<sup>36</sup> prediction for a rotational discontinuity. The outflow velocity reaching the Alfvén speed in guide field reconnection is consistent with the physics leading to Eq. (11). In the presence of a strong guide field, the firehose instability is suppressed in the reconnection exhaust, leaving the reconnected field lines' tension force intact.

Finally, we estimate the strength of the guide field required to transition from firehose unstable to stable. The firehose instability will be suppressed when the guide field in the exhaust is large enough to keep  $\epsilon \geq 0$ . Neglecting the reconnecting component of the magnetic field in the exhaust and compressional effects in the exhaust, this translates to  $\frac{B_g^2}{8\pi n} \geq \Delta T_{i\parallel} - \Delta T_{i\perp}$ . The difference in heating can be estimated from observations and simulations where the total ion heating is found to be  $(\Delta T_{i\parallel} + 2\Delta T_{i\perp})/3 \sim 0.125 \frac{B_r^2}{4\pi n}$  and  $\Delta T_{i\parallel} \approx 2\Delta T_{i\perp}$ .<sup>12,18</sup> This can be rearranged as  $\Delta T_{i\parallel} - \Delta T_{i\perp} \approx 0.094 m_i c_{Ar}^2$ . Substituting in the difference in heating, we find that firehose instability should be approximately suppressed for  $B_g \approx 0.43 B_r$  which corresponds to an approximate shear angle of 135°. This value is consistent with the transition found in simulations and serves as a natural value to separate nearly anti-parallel and guide field reconnection.

#### IV. DISCUSSION AND CONCLUSION

We have shown in simulations and observations that there is a systematic reduction of the outflow velocity in nearly anti-parallel magnetic reconnection events. The reduction of the outflow velocity is correlated with the ion temperature and is shown to be due to the firehose instability in the exhaust. The outflow velocity is shown to be well predicted by  $v_0 = c_{Ar}^2 / (3\sqrt{T_{i\parallel}/m_i})$ . It is also shown that for events with a sufficiently strong guide field (with strength

comparable to the reconnecting magnetic field) that the outflow velocity reaches the Alfvén speed. The clear agreement between the theory proposed in this paper with the simulations and observations strengthens the claim that the firehose instability in reconnection exhausts is responsible for the reduction of the outflow velocity.

This result has significant implications for an important open question about the nature of collisionless magnetic reconnection: What is the partition of converted magnetic energy? The bulk outflow contains a significant fraction of the released magnetic energy<sup>14,16,17,42</sup> and so if the outflow velocity is reduced and the total magnetic energy released remains the same, then more energy will be released into other degrees of freedom. Therefore, the relationship between exhaust ion temperature and outflow velocity described here is an important step towards a predictive model of the partition of reconnection energy.

#### SUPPLEMENTARY MATERIAL

See [supplementary material](#) for the initial parameters of the 81 different PIC simulations used in this study, where  $m_i/m_e$  is the artificial ion to electron mass ratio,  $B_r$  is the magnitude of the reconnection component of the upstream magnetic field,  $B_g$  is the upstream component of the magnetic field normal to the current sheet and the outflow direction called the guide field,  $n_{in}$  is the initial upstream density,  $T_e$  and  $T_i$  are the initial electron and ion temperature, respectively, and  $\beta_r$  is the total plasma beta based on the reconnecting component of the magnetic field.

#### ACKNOWLEDGMENTS

This research was supported by NSF under Grant Nos. AGS-1460130 and AGS-1460037 as well as NASA under Grant Nos. NNX08A083G (MMS IDS), NNX14AC39G (MMS Theory and Modeling team), NNX15AW58G, NNX16AF75G, NNX16AG76G, and NNX17AI25G, and Thailand Research Fund under Grant No. RTA5980003. Simulations and analysis were performed at the National Center for Atmospheric Research Computational and Information Systems Laboratory (NCAR-CISL) and at the National Energy Research Scientific Computing Center (NERSC). Rungployphan Kieokaew acknowledges financial support from the Faculty of Science at Mahidol University on short-term research overseas to visit Bartol Research Institute.

<sup>1</sup>E. Priest and T. Forbes, *Magnetic Reconnection, MHD Theory and Applications* (Cambridge University Press, New York, NY, 2000).

<sup>2</sup>E. N. Parker, *J. Geophys. Res.* **62**, 509, <https://doi.org/10.1029/JZ062i004p00509> (1957).

<sup>3</sup>G. Paschmann, I. Papamastorakis, N. Sckopke, G. Haerendel, B. U. Ö. Sonnerup, S. J. Bame, J. R. Asbridge, J. T. Gosling, C. T. Russel, and R. C. Elphic, *Nature* **282**, 243 (1979).

<sup>4</sup>B. U. Sonnerup, *J. Geophys. Res.* **86**, 10049, <https://doi.org/10.1029/JA086iA12p10049> (1981).

<sup>5</sup>T. Sato and T. Hayashi, *Phys. Fluids* **22**, 1189 (1979).

<sup>6</sup>J. Birn and J. E. W. Hones, *J. Geophys. Res.* **86**, 6802, <https://doi.org/10.1029/JA086iA08p06802> (1981).

<sup>7</sup>R. L. Stenzel, W. Gekelman, and N. Wild, *J. Geophys. Res.* **87**, 111, <https://doi.org/10.1029/JA087iA01p00111> (1982).

- <sup>8</sup>G. Paschmann, W. Baumjohann, N. Sckopke, I. Papamastorakis, and C. W. Carlson, *J. Geophys. Res.* **91**, 11099, <https://doi.org/10.1029/JA091iA10p11099> (1986).
- <sup>9</sup>T.-D. Phan, G. Paschmann, and B. U. Sonnerup, *J. Geophys. Res.* **101**, 7817, <https://doi.org/10.1029/95JA03751> (1996).
- <sup>10</sup>J. T. Gosling, S. Eriksson, T. D. Phan, D. E. Larson, R. M. Skoug, and D. J. McComas, *Geophys. Res. Lett.* **34**, L06102 <https://doi.org/10.1029/2006GL029033> (2007).
- <sup>11</sup>Y.-H. Liu, J. F. Drake, and M. Swisdak, *Phys. Plasmas* **19**, 22110 (2012).
- <sup>12</sup>C. C. Haggerty, M. A. Shay, J. F. Drake, T. D. Phan, and C. T. McHugh, *Geophys. Res. Lett.* **42**, 9657, <https://doi.org/10.1002/2015GL065961> (2015).
- <sup>13</sup>J. F. Drake, M. Swisdak, T. D. Phan, P. A. Cassak, M. A. Shay, S. T. Lepri, R. P. Lin, E. Quataert, and T. H. Zurbuchen, *J. Geophys. Res.* **114**, A051111, <https://doi.org/10.1029/2008JA013701> (2009).
- <sup>14</sup>J. P. Eastwood, T. D. Phan, J. F. Drake, M. A. Shay, A. L. Borg, B. Lavraud, and M. G. G. T. Taylor, *Phys. Rev. Lett.* **110**, 225001 (2013).
- <sup>15</sup>G. Lapenta, M. Goldman, D. Newman, S. Markidis, and A. Divin, *Phys. Plasmas* **21**, 055702 (2014).
- <sup>16</sup>M. Yamada, J. Yoo, J. Jara-Almonte, H. Ji, R. M. Kulsrud, and C. E. Myers, *Nat. Commun.* **5**, 4774 (2014).
- <sup>17</sup>M. A. Shay, C. C. Haggerty, T. D. Phan, J. F. Drake, P. A. Cassak, P. Wu, M. Oieroset, M. Swisdak, and K. Malakit, *Phys. Plasmas* **21**, 122902 (2014).
- <sup>18</sup>T. D. Phan, M. A. Shay, J. T. Gosling, M. Fujimoto, J. F. Drake, G. Paschmann, M. Oieroset, J. P. Eastwood, and V. Angelopoulos, *Geophys. Res. Lett.* **40**, 4475, <https://doi.org/10.1002/grl.50917> (2013).
- <sup>19</sup>H. S. Fu, J. B. Cao, Y. V. Khotyaintsev, M. I. Sitnov, A. Runov, S. Y. Fu, M. Hamrin, M. André, A. Retinò, Y. D. Ma, H. Y. Lu, X. H. Wei, and S. Y. Huang, *Geophys. Res. Lett.* **40**, 6023, <https://doi.org/10.1002/2013GL058620> (2013).
- <sup>20</sup>P. L. Pritchett, *Earth, Planets Space* **67**, 103 (2015).
- <sup>21</sup>J. F. Drake, M. Swisdak, K. M. Schoeffler, B. N. Rogers, and S. Kobayashi, *Geophys. Res. Lett.* **33**, L13105, <https://doi.org/10.1029/2006GL025957> (2006).
- <sup>22</sup>J. T. Dahlin, J. F. Drake, and M. Swisdak, *Phys. Plasmas* **21**, 92304 (2014).
- <sup>23</sup>J. T. Dahlin, J. F. Drake, and M. Swisdak, *Phys. Plasmas* **22**, 100704 (2015).
- <sup>24</sup>Y.-H. Liu, J. F. Drake, and M. Swisdak, *Phys. Plasmas* **18**, 92102 (2011).
- <sup>25</sup>A. Zeiler, D. Biskamp, J. F. Drake, B. N. Rogers, M. A. Shay, and M. Scholer, *J. Geophys. Res.* **107**, 1230, <https://doi.org/10.1029/2001JA000287> (2002).
- <sup>26</sup>J. T. Gosling, R. M. Skoug, D. J. McComas, and C. W. Smith, *Geophys. Res. Lett.* **110**, A01107, <https://doi.org/10.1029/2004JA010809> (2005).
- <sup>27</sup>J. T. Gosling, S. Eriksson, R. M. Skoug, D. J. McComas, and R. J. Forsyth, *Astrophys. J.* **644**, 613 (2006).
- <sup>28</sup>M. S. Davis, T. D. Phan, J. T. Gosling, and R. M. Skoug, *Geophys. Res. Lett.* **33**, L19102, <https://doi.org/10.1029/2006GL026735> (2006).
- <sup>29</sup>T. D. Phan, G. Paschmann, C. Twitty, F. S. Mozer, J. T. Gosling, J. P. Eastwood, M. Oieroset, H. Rème, and E. A. Lucek, *Geophys. Res. Lett.* **34**, L14104, <https://doi.org/10.1029/2007GL030343> (2007).
- <sup>30</sup>T. D. Phan, J. T. Gosling, and M. S. Davis, *Geophys. Res. Lett.* **36**, L09108, <https://doi.org/10.1029/2009GL037713> (2009).
- <sup>31</sup>H. Hietala, J. F. Drake, T. D. Phan, J. P. Eastwood, and J. P. McFadden, *Geophys. Res. Lett.* **42**, 7239, <https://doi.org/10.1002/2015GL065168> (2015).
- <sup>32</sup>M. Oieroset, T. D. Phan, C. Haggerty, M. A. Shay, J. P. Eastwood, D. J. Gershman, J. F. Drake, M. Fujimoto, R. E. Ergun, F. S. Mozer, M. Oka, R. B. Torbert, J. L. Burch, S. Wang, L. J. Chen, M. Swisdak, C. Pollock, J. C. Dorelli, S. A. Fuselier, B. Lavraud, B. L. Giles, T. E. Moore, Y. Saito, L. A. Avanov, W. Paterson, R. J. Strangeway, C. T. Russell, Y. Khotyaintsev, P. A. Lindqvist, and K. Malakit, *Geophys. Res. Lett.* **43**, 5536, <https://doi.org/10.1002/2016GL069166> (2016).
- <sup>33</sup>M. Oieroset, T. Phan, M. Shay, C. Haggerty, M. Fujimoto, V. Angelopoulos, J. Eastwood, and F. Mozer, *Geophys. Res. Lett.* **44**, 7598, <https://doi.org/10.1002/2017GL074196> (2017).
- <sup>34</sup>G. F. Chew, M. L. Goldberger, and F. E. Low, *Proc. R. Soc. A* **236**, 112 (1956).
- <sup>35</sup>E. N. Parker, *Phys. Rev.* **109**, 1874 (1958).
- <sup>36</sup>P. D. Hudson, *Planet. Space Sci.* **18**, 1611 (1970).
- <sup>37</sup>M. A. Shay, J. F. Drake, B. N. Rogers, and R. E. Denton, *J. Geophys. Res.* **106**, 3759, <https://doi.org/10.1029/1999JA001007> (2001).
- <sup>38</sup>R. Mistry, J. Eastwood, C. Haggerty, M. Shay, T. Phan, H. Hietala, and P. Cassak, *Phys. Rev. Lett.* **117**, 185102 (2016).
- <sup>39</sup>A. Le, J. Egedal, W. Daughton, W. Fox, and N. Katz, *Phys. Rev. Lett.* **102**, 85001 (2009).
- <sup>40</sup>J. Egedal, W. Fox, N. Katz, M. Porkolab, M. Oieroset, R. P. Lin, W. Daughton, and J. F. Drake, *J. Geophys. Res. (Space Phys.)* **113**, A12207, <https://doi.org/10.1029/2008JA013520> (2008).
- <sup>41</sup>T. D. Phan, J. F. Drake, M. A. Shay, J. T. Gosling, G. Paschmann, J. P. Eastwood, M. Oieroset, M. Fujimoto, and V. Angelopoulos, *Geophys. Res. Lett.* **41**, 7002, <https://doi.org/10.1002/2014GL061547> (2014).
- <sup>42</sup>J. Birn, J. E. Borovsky, M. Hesse, and K. Schindler, *Phys. Plasmas* **17**, 052108 (2010).